


Heavy-quark expansion for lifetimes: Toward the QCD corrections to power suppressed terms

Thomas Mannel,¹ Daniel Moreno^{1,2}, and Alexei A. Pivovarov¹

¹Center for Particle Physics Siegen, Theoretische Physik 1, Universität Siegen 57068 Siegen, Germany

²Paul Scherrer Institut, CH-5232 Villigen PSI, Switzerland

 (Received 25 April 2023; accepted 30 May 2023; published 20 June 2023)

We consider the heavy-quark expansion for the nonleptonic decay rates of heavy hadrons, and compute the next-to-leading-order QCD corrections to power terms up to order $1/m_Q^2$. We neglect the masses of the final-state quarks, so the application of our result is mainly for charmed hadrons. Our result can be applied also to bottomed hadrons as they constitute the main effect to this order up to corrections of $\mathcal{O}(m_c/m_b)$ and contributions due to penguin operators. We discuss the impact of our result for the lifetimes of heavy hadrons.

DOI: [10.1103/PhysRevD.107.114026](https://doi.org/10.1103/PhysRevD.107.114026)

I. INTRODUCTION

With the development of the heavy-quark expansion (HQE) [1–4], the theoretical description of inclusive decay rates of heavy hadrons (i.e. of hadrons containing a single heavy-quark Q) has been advanced significantly. The HQE allows us to describe their decay rates Γ and spectra as a systematic expansion of the form [5–9]

$$\Gamma = \sum_{n=0}^{\infty} \Gamma_n \left(\frac{1}{m_Q} \right)^n, \quad (1)$$

where the $\Gamma_n \propto \Lambda_{\text{QCD}}^n$ involve nonperturbative parameters, the so-called HQE parameters, with coefficients that can be computed perturbatively as a power series in $\alpha_s(m_Q)$.

Over the last decades, this method has been continuously improved and refined, in particular by computing higher-order corrections in Λ_{QCD}/m_Q as well as higher orders in $\alpha_s(m_Q)$. For inclusive semileptonic decays and motivated by the possibility to determine V_{cb} with high precision, the HQE has been investigated very intensively, while for inclusive nonleptonic rates the HQE has been pushed to a similar level.

The most inclusive quantities are the lifetimes of heavy hadrons, which can be computed in the HQE. Its main prediction is that the leading contribution to the heavy-hadron lifetime is described by the decay rate of the corresponding free heavy-quark. To this end, the HQE

thus predicts that all heavy-hadron lifetimes are equal up to corrections of order $(\Lambda_{\text{QCD}}/m_Q)^2$, since the term linear in the expansion parameter is absent due to heavy-quark symmetries. In fact this was an embarrassment in the early days of the HQE, since at that time only measurements of lifetimes of charmed hadrons were available. The current numbers are [10]

$$\begin{aligned} \frac{\tau(D^\pm)|^{\text{exp}}}{\tau(D^0)} &= 2.563 \pm 0.017, \\ \frac{\tau(D_s)|^{\text{exp}}}{\tau(D^0)} &= 1.219 \pm 0.017, \\ \frac{\tau(D^\pm)|^{\text{exp}}}{\tau(\Lambda_c)} &= 5.123 \pm 0.014, \end{aligned} \quad (2)$$

which are in contrast to the expectation of a few percent. This clearly shows that this simple picture is too naive in the case of the charm, leaving us with some doubt on the applicability of the HQE for the charm quark [11]. Within the HQE, the large lifetime differences are tracked by matrix elements of four-quark operators which have Wilson coefficients that are enhanced by a $16\pi^2$ phase-space factor and scale as $16\pi^2(\Lambda_{\text{QCD}}/m_c)^3$ relative to the leading term [12]. In the case of the charm, these terms can become comparable to the leading term. The successful applications of the HQE to the charm are all related to observables where the matrix elements of these four-quark operators are suppressed for some physical reason. The HQE for charmed hadrons have been extensively used to explore its applicability, e.g. in [13–17].

In contrast, for the bottom quark this picture seems to be more realistic, since one finds for the bottom hadrons [10]

Published by the American Physical Society under the terms of the [Creative Commons Attribution 4.0 International license](https://creativecommons.org/licenses/by/4.0/). Further distribution of this work must maintain attribution to the author(s) and the published article's title, journal citation, and DOI. Funded by SCOAP³.

$$\begin{aligned}
\left. \frac{\tau(B_s)}{\tau(B_d)} \right|_{\text{exp}} &= 0.998 \pm 0.004, \\
\left. \frac{\tau(B^+)}{\tau(B_d)} \right|_{\text{exp}} &= 1.076 \pm 0.004 \\
\left. \frac{\tau(\Lambda_b)}{\tau(B^+)} \right|_{\text{exp}} &= 0.969 \pm 0.006
\end{aligned} \tag{3}$$

which is a clear motivation for considering also higher-order corrections to the HQE of lifetimes, whose current status has been presented in [18–22].

As for the current knowledge of the perturbative QCD corrections to the coefficients of the HQE of the rate, the situation is the following:

- (i) Semileptonic decays: The leading power coefficient is known at next-to-next-to-next-to-leading order [23,24]. The coefficients of the first power correction are known at next-to-leading order (NLO) [25–27]. From the second power correction onward four-quark operators start to appear. For the second power correction the coefficients of the two-quark and four-quark operators are known at NLO [28–31]. Finally, the coefficients of the third and fourth power corrections are known at LO [32,33] for the two-quark operators.
- (ii) Nonleptonic decays: The leading power coefficient is known at NLO [34–37] and at NNLO in the massless case for the color-singlet $\Delta B = 1$ operator [38]. The coefficients of the first power correction are known at LO [6,39,40]. The coefficients of the second power correction are known at LO for the two-quark operators [41–43] and at NLO for the four-quark operators [44,45]. Finally, the coefficients of the third power correction are known at LO for the four-quark operators [46].

In the present paper we extend the existing calculations for nonleptonic widths by computing α_s corrections to power suppressed terms at next-to-leading power. We present an analytical result for the nonleptonic width at order $\alpha_s(m_Q)(\Lambda_{\text{QCD}}/m_Q)^2$ for the case of vanishing final-state quark masses.

The main application of our result is D hadron decays as it corresponds to the Cabibbo-Kobayashi-Maskawa (CKM) favored decay channel $c \rightarrow s\bar{d}u$. To some extent, our results can be applied to B hadron decays. To order $\alpha_s(m_Q)(\Lambda_{\text{QCD}}/m_Q)^2$ they constitute the main effect in the CKM favored decay channel $b \rightarrow c\bar{u}d$ up to corrections of $\mathcal{O}(m_c/m_b)$. The same is true for the CKM favored decay channel $b \rightarrow c\bar{c}s$ up to corrections of $\mathcal{O}(m_c/m_b)$ and up to the effect of penguin operators, which is not considered in this paper.

The paper is organized as follows. In Sec. II we discuss the effective electroweak Lagrangian and the choice of the renormalization scheme. In Sec. III we set the definitions

for the HQE. In Sec. IV we describe our method for the computation. Finally, we collect the results and discuss their impact in Sec. V.

II. THE EFFECTIVE ELECTROWEAK LAGRANGIAN

In this section we discuss the effective Lagrangian describing nonleptonic transitions and provide the main definitions needed for this paper. At low momentum transfer compared to the W -boson mass M_W , the nonleptonic heavy-quark decay $Q \rightarrow q_1\bar{q}_2q_3$ can be described by an effective Fermi Lagrangian

$$\mathcal{L}_{\text{eff}} = -2\sqrt{2}G_F V_{q_2q_3} V_{q_1Q}^* (C_1 \mathcal{O}_1 + C_2 \mathcal{O}_2) + \text{H.c.}, \tag{4}$$

where G_F is the Fermi constant, $V_{qq'}$ are the corresponding matrix elements of the CKM matrix and $C_{1,2}$ are matching coefficients. We start from the standard operator basis $\mathcal{O}_{1,2}$ with color singlet and color rearranged operators [47]

$$\mathcal{O}_1 = (\bar{Q}^i \Gamma_\mu q_1^j) (\bar{q}_2^j \Gamma^\mu q_3^i), \tag{5}$$

$$\mathcal{O}_2 = (\bar{Q}^i \Gamma_\mu q_1^i) (\bar{q}_2^j \Gamma^\mu q_3^j), \tag{6}$$

where $\Gamma_\mu = \gamma_\mu(1 - \gamma_5)/2 = \gamma_\mu P_L$, (i, j) are color indices, and $q_{1,2,3}$ are the final-state quarks which we take to be massless in the following. We assume for simplicity that the three final-state quarks have different flavors, so we do not need to consider QCD penguin operators.

However, for the calculation we address in this paper, it is convenient to choose a different operator basis for our effective Lagrangian in Eq. (4)

$$\mathcal{L}_{\text{eff}} = -2\sqrt{2}G_F V_{q_2q_3} V_{q_1Q}^* (C_+ \mathcal{O}_+ + C_- \mathcal{O}_-) + \text{H.c.}, \tag{7}$$

with $\mathcal{O}_\pm = (\mathcal{O}_2 \pm \mathcal{O}_1)/2$ and $C_\pm = C_2 \pm C_1$. The advantage is that this basis is diagonal under renormalization. In the $\overline{\text{MS}}$ renormalization scheme

$$\begin{aligned}
C_{\pm,B} &= Z_\pm C_\pm, & Z_\pm &= 1 + \frac{1}{2} \gamma_\pm \frac{\alpha_s(\mu)}{4\pi} \frac{1}{\epsilon}, \\
\gamma_\pm &= -6 \left(\frac{1}{N_c} \mp 1 \right),
\end{aligned} \tag{8}$$

where the subindex B stands for bare quantities and those without subscript stand for renormalized ones, $N_c = 3$ is the number of colors and γ_\pm is the LO anomalous dimension of the operators \mathcal{O}_\pm .

An important technical issue here is to retain the same scheme for the calculation of correlators and for the calculation of the short-distance Wilson coefficients C_\pm appearing in the effective Lagrangian. The point is that the renormalization of the operators \mathcal{O}_\pm is additionally complicated by the fact that they involve left-handed fields

and require the special treatment of γ_5 in dimensional regularization. There are several possibilities like dimensional reduction [34], the 't Hooft–Veltman scheme [35], or naive dimensional regularization (NDR) with anticommuting γ_5 [36].

We decide to closely follow the approach used by [36] and chose to work in NDR within the scheme of evanescent operators that preserves Fierz symmetry [47–53]. Such evanescent operators are defined in Ref. [47], where the two-loop anomalous dimension required for the running of C_\pm at NLO is also computed. This definition respects the Fierz transformation which in general is valid only in four-dimensional space-time. This choice is very handy as it allows us, by using an appropriate Fierz transformation, to avoid closed fermionic loops, which are known to lead to algebraic inconsistencies when using anticommuting γ_5 in D dimensions.

The freedom in the choice of evanescent operators is connected with the freedom in the choice of the renormalization scheme. Such a freedom is represented by the shift

$$A\gamma_\pm = A\left(\pm 1 + \frac{1}{N_c}\right), \quad (9)$$

proportional to the LO anomalous dimensions γ_\pm of the operators \mathcal{O}_\pm .

In the following we give the definition for the coefficients C_\pm in NDR within the scheme of evanescent operators that preserves Fierz symmetry. The Wilson coefficients C_\pm with NLO precision (including also the renormalization group improvement at NLO) are given by [34,36,47]

$$C_\pm(\mu) = L_\pm(\mu) \left[1 + \frac{\alpha_s(M_W) - \alpha_s(\mu)}{4\pi} R_\pm + \frac{\alpha_s(\mu)}{4\pi} B_\pm \right], \quad (10)$$

which have been calculated at the scale $\mu = M_W$ and then evolved down to scales $\mu \ll M_W$ by solving the corresponding renormalization group equations. The equation above splits the coefficients into a scheme-independent part proportional to R_\pm and a scheme-dependent part proportional to B_\pm , with [34–36,47]

$$\begin{aligned} R_+ &= \frac{10863 - 1278n_f + 80n_f^2}{6(33 - 2n_f)^2}, \\ R_- &= -\frac{15021 - 1530n_f + 80n_f^2}{3(33 - 2n_f)^2}, \\ B_\pm &= \frac{1}{12} B\gamma_\pm, \end{aligned} \quad (11)$$

where n_f is the number of light flavors and $B = 11$ in NDR with anticommuting γ_5 [47]. The last equation is implied by Fierz symmetry. The matching coefficients B_\pm ensure that, up to terms of order $\alpha_s^2(M_W)$, matrix elements of the

effective Lagrangian calculated at the scale $\mu = M_W$ are equal to the corresponding matrix elements calculated with the full standard model Lagrangian. Eventually, the scheme dependence absorbed in B_\pm has to cancel against the scheme dependence of matrix elements of the corresponding operators.

Finally,

$$L_\pm(\mu) = \left(\frac{\alpha_s(M_W)}{\alpha_s(\mu)} \right)^{\frac{\gamma_\pm}{2\beta_0}} \quad (12)$$

is the solution of the renormalization group equation (RGE) for C_\pm to leading logarithmic accuracy, with $\beta_0 = \frac{11}{3}N_c - \frac{2}{3}n_f$.

III. HQE FOR NONLEPTONIC DECAYS OF HEAVY FLAVORS

This section briefly describes the theoretical framework used for the calculation of inclusive nonleptonic decays of heavy hadrons within the HQE and provides the main definitions. We follow the approach introduced in [26,27,30].

By using the optical theorem one obtains the inclusive decay rate Γ from taking an absorptive part of the forward matrix element of the leading-order transition operator \mathcal{T} ,

$$\begin{aligned} \mathcal{T} &= i \int d^4x T \{ \mathcal{L}_{\text{eff}}(x) \mathcal{L}_{\text{eff}}(0) \}, \\ \Gamma(H_Q \rightarrow X) &= \frac{1}{M_{H_Q}} \text{Im} \langle H_Q | \mathcal{T} | H_Q \rangle, \end{aligned} \quad (13)$$

where M_{H_Q} is the heavy-hadron mass and $|H_Q\rangle$ its quantum state. Since the heavy-quark mass m_Q is a large scale compared to the QCD hadronization scale Λ_{QCD} ($m_Q \gg \Lambda_{\text{QCD}}$), the forward matrix element contains perturbatively calculable contributions. These can be separated from the nonperturbative pieces using the method of effective field theory. For a heavy hadron with momentum p_{H_Q} and mass M_{H_Q} , a large part of the heavy-quark momentum p_Q originates from a pure kinematical contribution due to its large mass. We split the heavy-quark momentum according to $p_Q = m_Q v + \Delta$ with $v = p_{H_Q}/M_{H_Q}$ being the velocity of the heavy hadron. The residual momentum $\Delta \sim \mathcal{O}(\Lambda_{\text{QCD}})$ describes the soft-scale fluctuations of the heavy-quark field near its mass shell.

This decomposition of the quark momentum is implemented by redefining the heavy-quark field according to

$$Q(x) = e^{-im_Q v \cdot x} \mathcal{Q}_v(x), \quad (14)$$

so that $i\partial \mathcal{Q}_v(x) \sim \Delta$.

We set up the HQE as an expansion in Λ_{QCD}/m_Q by matching the transition operator \mathcal{T} in QCD to an expansion in inverse powers of the heavy-quark mass, using operators defined in heavy-quark effective theory (HQET) [54–57].

Generally, the HQE for heavy-hadron weak decays takes the form

$$\Gamma(H_Q \rightarrow X) = \Gamma^0 |V_{q_2 q_3}|^2 |V_{q_1 Q}|^2 \times \left(C_0 - C_{\mu_\pi} \frac{\mu_\pi^2}{2m_Q^2} + C_{\mu_G} \frac{\mu_G^2}{2m_Q^2} + \dots \right), \quad (15)$$

where $\Gamma^0 = G_F^2 m_Q^5 / (192\pi^3)$ and the ellipsis denotes terms of order $1/m_Q^n$, $n \geq 3$. The coefficients C_0 , C_{μ_π} , and C_{μ_G} can be computed as a power series in $\alpha_s(\mu)$ and depend, in case of neglecting the final-state quark masses, on logarithms of μ/m_Q , where μ is the matching scale. Therefore, for $\mu = m_Q$ the coefficients are pure numbers. The parameters μ_π^2 , μ_G^2 are forward matrix elements of local HQET operators called HQE parameters.

The previous expression emerges from the direct matching of the QCD expression for the transition operator to HQET

$$\text{Im}\mathcal{T} = \Gamma^0 |V_{q_2 q_3}|^2 |V_{q_1 Q}|^2 \left(C_0 \mathcal{O}_0 + C_v \frac{\mathcal{O}_v}{m_Q} + C_\pi \frac{\mathcal{O}_\pi}{2m_Q^2} + C_G \frac{\mathcal{O}_G}{2m_Q^2} + \dots \right), \quad (16)$$

where again the coefficients C_0 , C_v , C_π and C_G can be computed as a power series in $\alpha_s(\mu)$. The local operators \mathcal{O}_i in the equation above are ordered by their mass dimensionality and are given by¹

$$\mathcal{O}_0 = \bar{h}_v h_v \quad (\text{mass dimension three}), \quad (17)$$

$$\mathcal{O}_v = \bar{h}_v v \cdot \pi h_v \quad (\text{mass dimension four}), \quad (18)$$

$$\mathcal{O}_\pi = \bar{h}_v \pi_\perp^2 h_v \quad (\text{mass dimension five}), \quad (19)$$

$$\mathcal{O}_G = \frac{1}{2} \bar{h}_v [\gamma^\mu, \gamma^\nu] \pi_{\perp\mu} \pi_{\perp\nu} h_v \quad (\text{mass dimension five}), \quad (20)$$

where $\pi_\mu = iD_\mu = i\partial_\mu + g_s A_\mu^a T^a$ is the covariant derivative of QCD and $\pi^\mu = v^\mu (v\pi) + \pi_\perp^\mu$.

Note that the field h_v denotes the static quark field moving with the velocity v as defined in HQET. Furthermore, it is convenient to trade the leading term operator \mathcal{O}_0 in Eq. (16) by the local QCD operator $\bar{Q}\not{v}Q$, since its forward hadronic matrix element is normalized to unity. Expanding $\bar{Q}\not{v}Q$ up to the desired order in $1/m_Q$ we get

¹In general, there is an additional operator $\mathcal{O}_1 = \bar{h}_v (v \cdot \pi)^2 h_v$ in the complete basis at dimension five. However it will be of higher order in the HQE after using the equations of motion of HQET.

$$\bar{Q}\not{v}Q = \mathcal{O}_0 + \tilde{C}_v \frac{\mathcal{O}_v}{m_Q} + \tilde{C}_\pi \frac{\mathcal{O}_\pi}{2m_Q^2} + \tilde{C}_G \frac{\mathcal{O}_G}{2m_Q^2} + \dots, \quad (21)$$

where \tilde{C}_i are the matching coefficients of the full QCD current to HQET.

Finally, we use the equation of motion (EOM) of the h_v field to remove the operator \mathcal{O}_v in Eq. (16)

$$\mathcal{O}_v = -\frac{1}{2m_Q} (\mathcal{O}_\pi + c_F(\mu) \mathcal{O}_G) + \dots, \quad (22)$$

where $c_F(\mu)$ is the chromomagnetic operator coefficient of the HQET Lagrangian

$$c_F(\mu) = 1 + \frac{\alpha_s(\mu)}{2\pi} \left[\frac{N_c^2 - 1}{2N_c} + N_c \left(1 + \ln \left(\frac{\mu}{m_Q} \right) \right) \right]. \quad (23)$$

In order to obtain the total rate, we have to take the forward matrix element of Eq. (16). For this we use the full QCD states $|H_Q(p_{H_Q})\rangle$, where H_Q is the 0^- ground state meson with a single heavy-quark Q . This introduces a dependence of the HQE parameters on the quark mass m_Q through the states which is nevertheless irrelevant to the order we are working on. The HQE parameters are defined as [58]

$$\langle H_Q(p_{H_Q}) | \bar{Q}\not{v}Q | H_Q(p_{H_Q}) \rangle = 2M_{H_Q}, \quad (24)$$

$$-\langle H_Q(p_{H_Q}) | \mathcal{O}_\pi | H_Q(p_{H_Q}) \rangle = 2M_{H_Q} \mu_\pi^2, \quad (25)$$

$$c_F(\mu) \langle H_Q(p_{H_Q}) | \mathcal{O}_G | H_Q(p_{H_Q}) \rangle = 2M_{H_Q} \mu_G^2, \quad (26)$$

where we have included $c_F(\mu)$ in the definition of the matrix element μ_G^2 in order to make the HQE parameters independent of the renormalization scale μ . Note that one may relate μ_G^2 to the mass splitting between the ground state mesons H and H^* ,

$$\mu_G^2 = \frac{3}{4} \Delta M_H^2 = \frac{3}{4} (M_{H^*}^2 - M_H^2). \quad (27)$$

IV. OUTLINE OF THE CALCULATION

The first step is to insert the effective Lagrangian Eq. (7) into the optical theorem Eq. (13) to perform the operator product expansion and obtain the total rate in the form of Eq. (15). In terms of the coefficients obtained from the matching calculation Eqs. (16) and (21), in combination with the EOM Eq. (22), we get

$$\Gamma(H_Q \rightarrow X) = \Gamma^0 |V_{q_2 q_3}|^2 |V_{q_1 Q}|^2 \left[C_0 \left(1 - \frac{\bar{C}_\pi - \bar{C}_v}{C_0} \frac{\mu_\pi^2}{2m_Q^2} \right) + \left(\frac{\bar{C}_G}{c_F(\mu)} - \bar{C}_v \right) \frac{\mu_G^2}{2m_Q^2} + \dots \right], \quad (28)$$

where we have defined $\bar{C}_i \equiv C_i - C_0 \tilde{C}_i$ as the difference between the coefficients of the HQE of the transition operator and the current multiplied by C_0 .

The computation of the coefficients follows our previous work [30,31] where we take the corresponding Feynman amplitude, expand to the necessary order in the small momentum k , and project to the corresponding HQET operators Eqs. (17), (18) and (20).

The Feynman diagrams contributing to the leading power coefficient C_0 at LO QCD and NLO QCD are two-loop and three-loop quark to quark self-energy-like diagrams. The ones contributing to the coefficients of power corrections \bar{C}_v and \bar{C}_G at LO QCD and NLO QCD are two-loop and three-loop quark to quark-gluon scattering diagrams.

The Feynman diagrams contributing to the coefficients C_0 , \bar{C}_v and \bar{C}_G of the HQE of the nonleptonic decay rate up to NLO are shown in Fig. 1. For the computation of the leading power coefficient C_0 only Figs. 1(a)–1(p) without gluon insertions have to be considered. For the computation of the next-to-leading-power coefficient \bar{C}_G and the auxiliary coefficient \bar{C}_v all diagrams [Figs. 1(a)–1(t)] containing

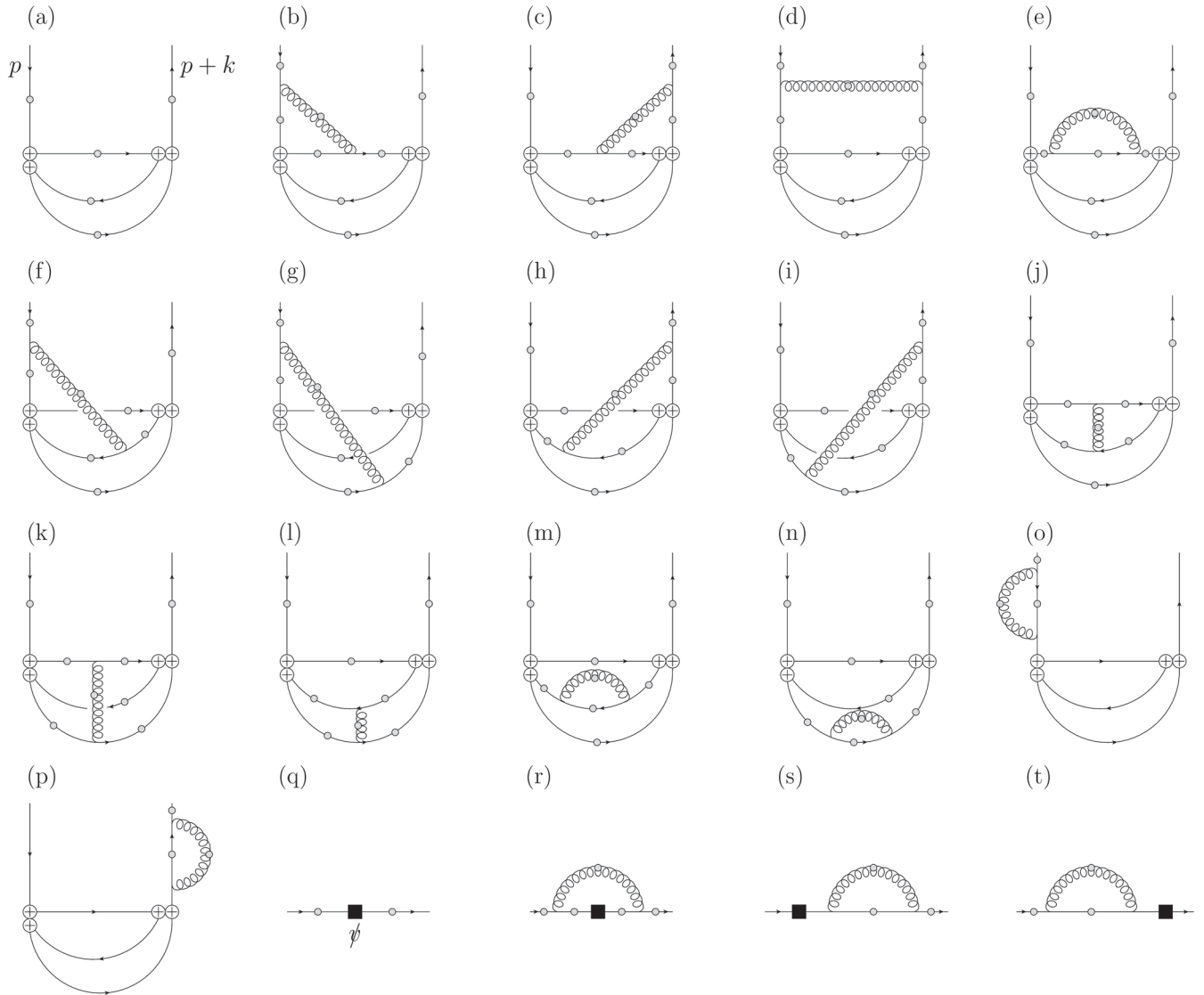


FIG. 1. Feynman diagrams (a)–(t) contributing to the coefficients C_0 , \bar{C}_v , and \bar{C}_G of the HQE of the nonleptonic decay rate up to NLO. The incoming heavy quark carries momentum p , with $p^2 = m_Q^2$. Grey dots stands for possible gluon insertions with incoming momentum $k \sim \Lambda_{\text{QCD}}$. The black box vertex stands for \not{p} insertions. All diagrams contributing to power corrections are obtained after taking into account all possible one-gluon insertions. Four-fermion vertices correspond to \mathcal{O}_\pm insertions of \mathcal{L}_{eff} .

one-gluon insertions have to be considered. Overall there are 14 diagrams contributing to C_0 up to NLO, one to LO and 13 to NLO. There are 128 diagrams contributing to \bar{C}_v and \bar{C}_G up to NLO, seven to LO and 121 to NLO.

By using LiteRed [59,60] the corresponding amplitudes are reduced to a combination of the master integrals given in Appendix A. The LO diagram Fig. 1(a) can be reduced to the two-loop master integral Fig. 4(a). Figures 1(a), 1(e), and 1(j)–1(n) can be reduced to a combination of the massless three-loop master integrals Figs. 4(b) and 4(c). Finally, Figs. 1(b)–1(d) and 1(f)–1(i) can be reduced to a combination of the massive three-loop master integrals Figs. 4(d) and 4(e).

We use standard dimensional regularization in $D=4-2\epsilon$ space-time dimensions with γ_5 treated in NDR. This forces us to choose a renormalization scheme with evanescent operators preserving Fierz symmetry to the necessary order. In this way, we can use Fierz symmetry to write all Feynman diagrams as a single open fermionic line without the γ_5 problem. Nevertheless, the explicit expressions for the coefficient functions of the HQE in terms of C_{\pm} are scheme dependent. This scheme dependence cancels with the corresponding scheme dependence of the coefficients C_{\pm} .

For the algebraic manipulations including Lorentz and Dirac algebra we use TRACER [61]. For the color algebra we use COLORMATH [62]. Expansion of hypergeometric functions is done with the help of HypExp [63,64]. The computation is performed in the Feynman gauge and we use the background field method to compute the scattering in the external gluonic field.

For renormalization we adopt the $\overline{\text{MS}}$ renormalization scheme for the strong coupling constant $\alpha_s(\mu)$ and the renormalization of the HQET Lagrangian. The heavy-quark is renormalized on shell

$$Q_B = (Z_2^{\text{ON}})^{1/2} Q, \quad Z_2^{\text{ON}} = 1 - \frac{N_c^2 - 1}{2N_c} \frac{\alpha_s}{4\pi} \left(\frac{3}{\epsilon} + 6 \ln \left(\frac{\mu}{m_Q} \right) + 4 \right). \quad (29)$$

Therefore, we will quote our results in the on-shell (pole mass) scheme for the heavy-quark mass m_Q . For the most precise predictions one usually chooses for the bottom quark a low-scale short-distance mass such as the kinetic or the $1S$ mass, and thus one needs to convert the on-shell mass into such a mass scheme for which the known one-loop expression will be sufficient.

V. RESULTS AND DISCUSSION

In this section we provide the results for the coefficients of the HQE of the nonleptonic decay rate in Eq. (15) up to NLO QCD. Note that the reparametrization invariance of the HQE ensures that to all orders in $\alpha_s(\mu)$ we have $C_0 = C_{\mu_\pi}$, so Eq. (15) takes the form

$$\Gamma(H_Q \rightarrow X) = \Gamma^0 |V_{q_2 q_3}|^2 |V_{q_1 Q}|^2 \times \left[C_0 \left(1 - \frac{\mu_\pi^2}{2m_Q^2} \right) + C_{\mu_G} \frac{\mu_G^2}{2m_Q^2} + \dots \right], \quad (30)$$

with

$$C_{\mu_G} = \frac{\bar{C}_G}{C_F(\mu)} - \bar{C}_v. \quad (31)$$

We show our results for the coefficients defined in Eq. (30) in the form

$$C_i = C_i^{\text{LO}} + \frac{\alpha_s(\mu)}{\pi} C_i^{\text{NLO}}, \quad i = 0, \mu_G. \quad (32)$$

The leading power coefficient reads

$$C_0^{\text{LO}} = \frac{1}{2} N_c (C_+^2 + C_-^2) + \frac{1}{2} (C_+^2 - C_-^2) = \frac{3}{2} (C_+^2 + C_-^2) + \frac{1}{2} (C_+^2 - C_-^2), \quad (33)$$

$$C_0^{\text{NLO}} = -(N_c^2 - 1) \left(\frac{\pi^2}{8} - \frac{31}{32} \right) (C_+^2 + C_-^2) - \frac{N_c^2 - 1}{2N_c} \left(\frac{3}{2} \ln \left(\frac{\mu^2}{m_Q^2} \right) + \frac{\pi^2}{4} + \frac{51}{16} \right) (C_+^2 - C_-^2) = - \left(\pi^2 - \frac{31}{4} \right) (C_+^2 + C_-^2) - \left(2 \ln \left(\frac{\mu^2}{m_Q^2} \right) + \frac{\pi^2}{3} + \frac{17}{4} \right) (C_+^2 - C_-^2), \quad (34)$$

while at subleading power we obtain

$$C_{\mu_G}^{\text{LO}} = -\frac{3}{2} N_c (C_+^2 + C_-^2) - \frac{19}{2} (C_+^2 - C_-^2) = -\frac{9}{2} (C_+^2 + C_-^2) - \frac{19}{2} (C_+^2 - C_-^2), \quad (35)$$

$$C_{\mu_G}^{\text{NLO}} = \left(12 \ln \left(\frac{\mu^2}{m_Q^2} \right) - \left(\frac{5}{288} + \frac{\pi^2}{8} \right) N_c^2 + \frac{31\pi^2}{24} + \frac{6533}{288} \right) (C_+^2 + C_-^2) + \frac{1}{N_c} \left(\frac{3}{4} (3N_c^2 - 19) \ln \left(\frac{\mu^2}{m_Q^2} \right) + \frac{13}{24} \left(\pi^2 - \frac{91}{12} \right) N_c^2 - \frac{179\pi^2}{72} - \frac{3361}{288} \right) (C_+^2 - C_-^2) = \left(12 \ln \left(\frac{\mu^2}{m_Q^2} \right) + \frac{\pi^2}{6} + \frac{811}{36} \right) (C_+^2 + C_-^2) + \left(2 \ln \left(\frac{\mu^2}{m_Q^2} \right) + \frac{43\pi^2}{54} - \frac{1751}{108} \right) (C_+^2 - C_-^2), \quad (36)$$

where in the second equalities we have replaced $N_c = 3$.

Note that the coefficient functions multiplying the C_{\pm} coefficients are in general dependent on the scheme used for γ_5 and the choice of evanescent operators. This scheme dependence cancels with the scheme dependence of the coefficients C_{\pm} . Therefore, the results written above together with the definitions given in Eqs. (10)–(12) are scheme independent. In addition we note that only two structures ($C_+^2 + C_-^2$) and ($C_+^2 - C_-^2$) appear. In the basis of Eq. (4) this is translated into the two structures ($C_1^2 + C_2^2$) and $C_1 C_2$. This is implied by Fierz symmetry.

The result obtained for the C_0 coefficient agrees with [36] which also was obtained in NDR and using Fierz symmetry. This result also agrees with [34,35], where this coefficient has been computed in dimensional reduction and the 't Hooft–Veltman scheme, respectively.

For the power suppressed terms, we recalculated the expression obtained for the C_{μ_G} coefficient, and our result agrees with the result known from [6,39,40]. The new result of this calculation is the next-to-leading-order contribution to the C_{μ_G} coefficient.

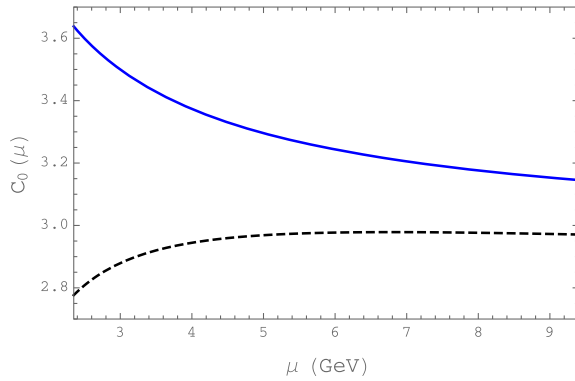
We may also switch to a reparametrization invariant basis as discussed in [58], where the HQE parameters are defined using the operators of full QCD as in Eq. (14)

$$\begin{aligned} & \langle H_Q(p_{H_Q}) | \bar{Q}_v Q_v | H_Q(p_{H_Q}) \rangle \\ & = 2M_{H_Q} \mu_3 = 2M_{H_Q} \left(1 - \frac{\mu_\pi^2 - \mu_G^2}{2m_Q^2} \right). \end{aligned} \quad (37)$$

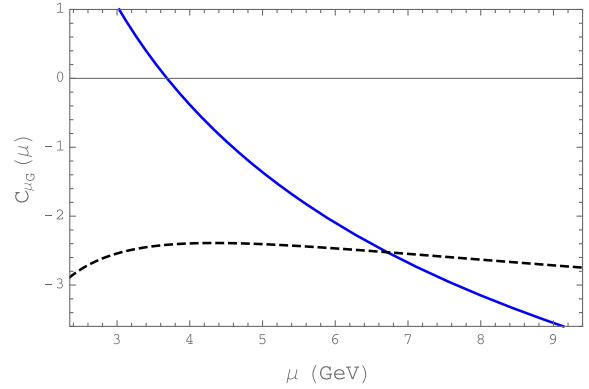
To the order we are working on we can identify the static field with the full QCD field, and find

$$\begin{aligned} \Gamma(H_Q \rightarrow X) & = \Gamma^0 |V_{q_2 q_3}|^2 |V_{q_1 Q}|^2 \\ & \times \left[C_0 \mu_3 + (C_{\mu_G} - C_0) \frac{\mu_G^2}{2m_Q^2} + \dots \right]. \end{aligned} \quad (38)$$

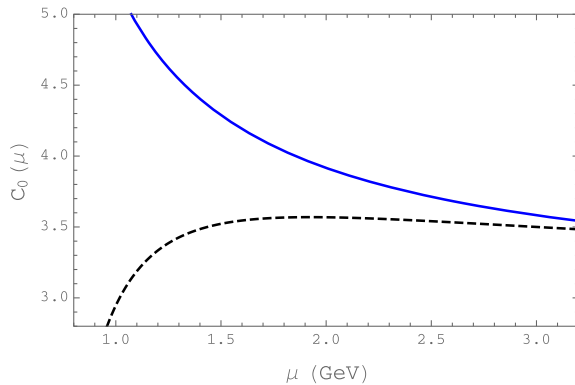
The NLO contributions to the coefficients are expected to reduce the dependence of the coefficients on the renormalization scale μ , so we look at the μ dependence of C_0 and C_{μ_G} . In Fig. 2 we show this dependence, varying μ in the range $m_Q/2 < \mu < 2m_Q$ for both the bottom- and



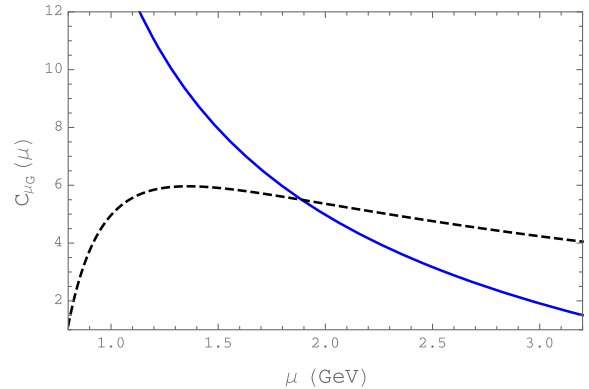
(a) C_0 for bottom quark case.



(b) C_{μ_G} for bottom quark case.



(c) C_0 for charm quark case.



(d) C_{μ_G} for charm quark case.

FIG. 2. The plots (a)–(d) show the dependence of the coefficients of the HQE of the inclusive nonleptonic decay rate on the renormalization scale μ in the range $m_Q/2 < \mu < 2m_Q$. The blue continuous lines stand for coefficients with LO precision whereas the black dashed lines stand for coefficients with NLO precision.

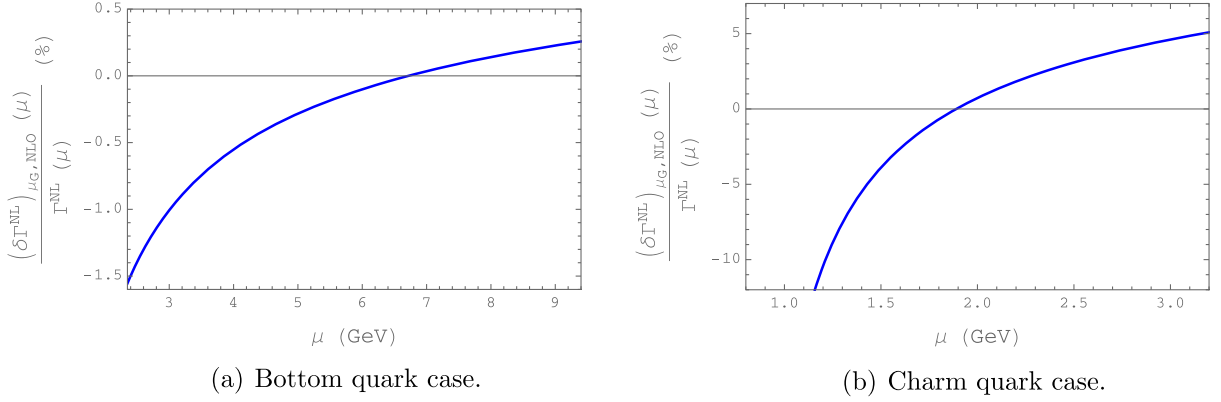


FIG. 3. Relative size between the new contribution to the nonleptonic width due to the NLO correction to the chromomagnetic operator coefficient $\delta\Gamma_{\mu_G, \text{NLO}}^{\text{NL}}(\mu)$ and the nonleptonic width $\Gamma^{\text{NL}}(\mu)$ as a function of the renormalization scale μ in the range $m_Q/2 < \mu < 2m_Q$. Panel (a) is the bottom-quark case and panel (b) is the charm-quark case.

the charm-quark cases. For illustration we take $m_b = 4.7 \text{ GeV}$, $m_c = 1.6 \text{ GeV}$, $M_Z = 91.18 \text{ GeV}$ and $\alpha_s(M_Z) = 0.118$, from which we obtain $\alpha_s(M_W) = 0.120$ at $M_W = 80.4 \text{ GeV}$. For the running of the strong coupling $\alpha_s(\mu)$ we use RUNDEC [65] to run it down from M_W to m_b with $n_f = 5$, and from m_b to m_c with $n_f = 4$. The two-loop running coupling is used.

As one would expect, the coefficients at NLO show a much weaker μ dependence than their LO counterparts. This is important phenomenologically since it will allow us to reduce the uncertainty due to the choice of the scale μ . This is especially true for the C_{μ_G} coefficient, where the uncertainty due to the choice of μ is very large.

As a consequence of the strong μ dependence of C_{μ_G} , NLO corrections to the C_{μ_G} coefficient are expected to be very large in general and should also strongly depend on the value of μ . The sum of LO and NLO contributions is, however, almost independent of μ . Therefore, NLO corrections happen to be very important and they stabilize the numerical value of the coefficient.

Note that for the bottom case, the leading-order chromomagnetic operator coefficient has a zero for a value of $\mu \approx 3.8 \text{ GeV}$, leading to a large uncertainty for this particular contribution. However, including the NLO contribution improves the situation significantly, leaving us with a negative contribution, lowering the total value of the width (increase the size of the lifetimes).

Finally we illustrate the impact of the new contribution to the nonleptonic width by looking at the quantity

$$\frac{\delta\Gamma_{\mu_G, \text{NLO}}^{\text{NL}}(\mu)}{\Gamma^{\text{NL}}(\mu)} \quad (39)$$

as a function of μ in the range $m_Q/2 < \mu < 2m_Q$. In Fig. 3 we show its μ dependence, inserting $\mu_G^2 = 0.35 \text{ GeV}^2$ and $\mu_\pi^2 = 0.5 \text{ GeV}^2$.

Based on this, we estimate a correction due to the new contribution to the nonleptonic width, and correspondingly to the lifetimes. We find a decrease of the rate of roughly $(-5 \pm 5)\%$ for the charm case, while the effect for the bottom case seems to be much smaller, roughly $(-0.5 \pm 0.5)\%$. However, the bottom case has to be taken with a grain of salt, since we did not take into account the $\mathcal{O}(m_c/m_b)$ effects.

VI. CONCLUSIONS

In this paper we have computed α_s corrections to the chromomagnetic operator coefficient in the HQE of the nonleptonic decay rate. This calculation represents the first attempt to include QCD corrections to power suppressed terms in nonleptonic decays. We have presented an analytical result for the nonleptonic width to order $\alpha_s(m_Q)(\Lambda_{\text{QCD}}/m_Q)^2$ for the case of vanishing final-state quark masses.

The main application of our result is for charm-hadron decays since our considerations correspond to the CKM favored decay channel $c \rightarrow s\bar{d}u$. To some extent, our results can be applied to B hadron decays. They constitute the main effect to order $\alpha_s(m_Q)(\Lambda_{\text{QCD}}/m_Q)^2$ in the CKM favored decay channel $b \rightarrow c\bar{u}d$ up to corrections of $\mathcal{O}(m_c/m_b)$. The same is true for the CKM favored decay channel $b \rightarrow c\bar{c}s$ up to corrections of $\mathcal{O}(m_c/m_b)$ and up to the effect of penguin operators, which have not been considered in this paper.

Our main result is that the inclusion of the NLO terms significantly reduces the dependence on the renormalization scale μ . While at leading order one finds a strong dependence, including the NLO terms turns out to have almost no μ dependence for the relevant range of μ . This stabilizes the numerical predictions significantly.

While our result can be directly applied to the case of the charm quark, where we can safely neglect the light quark masses, the case of the bottom quark is more involved,

since the charm-quark mass cannot be neglected and the coefficients will depend on m_c/m_b . It is known from the semileptonic case that the effects of the charm mass can be large. This will be subject of future investigations.

Finally we point out that the methods used here can be extended to the next power in $1/m_Q$, i.e. to a calculation of the NLO contribution to the Darwin operator coefficient, at least for the charm case where the final-state quarks can be treated as massless.

ACKNOWLEDGMENTS

We thank Alexander Lenz for fruitful discussions and his interest in this work. This research was supported by the Deutsche Forschungsgemeinschaft (DFG, German Research Foundation) under Grant No. 396021762—TRR 257 “Particle Physics Phenomenology after the Higgs Discovery.”

APPENDIX A: MASTER INTEGRALS

For completeness we give here the necessary master integrals for the computation of the coefficients of the HQE [66]. These master integrals are two- and three-loop $1 \rightarrow 1$ topologies with on-shell external momentum $p^2 = m_Q^2$.

1. Two-loop master integrals

We define the following completely massless two-loop basis:

$$\begin{aligned} D_1 &= (p - q_1)^2, & D_2 &= (p - q_2)^2, & D_3 &= q_1^2, \\ D_4 &= q_2^2, & D_5 &= (q_2 - q_1)^2. \end{aligned} \quad (\text{A1})$$

To LO, the most general integral that can appear is

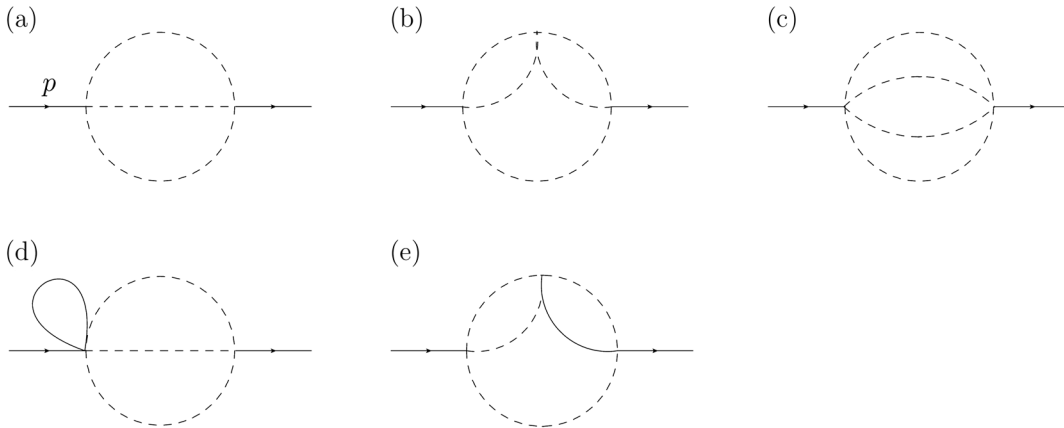


FIG. 4. Master integrals (a)–(e) contributing the matching coefficients of the HQE of inclusive nonleptonic decays. The dashed lines are massless whereas the continuous lines have mass m_Q .

$$\begin{aligned} \mathcal{J}(n_1, n_2, n_3, n_4, n_5) \\ = \text{Im} m_Q^{4\epsilon} \left(\frac{e^{\gamma_E}}{4\pi} \right)^{2\epsilon} \int \frac{d^D q_1}{(2\pi)^D} \int \frac{d^D q_2}{(2\pi)^D} \prod_{i=1}^5 \frac{1}{D_i^{n_i}}. \end{aligned} \quad (\text{A2})$$

After using integration by parts (IBP) reduction only one master integral appears which is represented in Fig. 4(a). It is a massless two-loop sunset topology. To the necessary order in the ϵ expansion it reads

$$\mathcal{J}(0, 1, 1, 0, 1) = \frac{m_Q^2}{512\pi^3} \left[1 + \frac{13}{2} \epsilon + \mathcal{O}(\epsilon^2) \right]. \quad (\text{A3})$$

2. Three-loop master integrals

We define the following three-loop basis with one massive denominator of mass m_Q :

$$\begin{aligned} D_1 &= (p - q_1)^2, & D_2 &= (p - q_2)^2, & D_3 &= (p - q_3)^2, \\ D_4 &= q_1^2, & D_5 &= q_2^2, & D_6 &= q_3^2 - m_Q^2, \\ D_7 &= (q_2 - q_1)^2, & D_8 &= (q_3 - q_2)^2, & D_9 &= (q_3 - q_1)^2. \end{aligned} \quad (\text{A4})$$

To NLO, the most general integral that can appear is

$$\begin{aligned} \mathcal{J}(n_1, \dots, n_9) &= \text{Im} m_Q^{6\epsilon} \left(\frac{e^{\gamma_E}}{4\pi} \right)^{3\epsilon} \frac{1}{i} \int \frac{d^D q_1}{(2\pi)^D} \int \frac{d^D q_2}{(2\pi)^D} \\ &\times \int \frac{d^D q_3}{(2\pi)^D} \prod_{i=1}^9 \frac{1}{D_i^{n_i}}. \end{aligned} \quad (\text{A5})$$

After using IBP reduction four master integrals appear. Two of them are the completely massless master integrals represented in Figs. 4(b) and 4(c) and the other two contain one massive line of mass m_Q and they are represented in Figs. 4(d) and 4(e). Figures 4(b) and 4(e) are five propagator topologies with zero and one massive lines, respectively. Figure 4(c) is a massless three-loop sunset

topology and Fig. 4(d) is a two-loop sunset topology with a massive tadpole of mass m_Q . The explicit expressions for the master integrals to the necessary order in the ϵ expansion are

$$\begin{aligned} & \mathcal{J}(0, 0, 1, 0, 1, 0, 1, 0, 1) \\ &= -\frac{m_Q^4}{49152\pi^5} \left[1 + \frac{71}{6}\epsilon + \left(\frac{3115}{36} - \frac{7\pi^2}{4} \right) \epsilon^2 + \mathcal{O}(\epsilon^3) \right], \end{aligned} \quad (\text{A6})$$

$$\begin{aligned} & \mathcal{J}(0, 0, 1, 1, 1, 0, 0, 1, 1) \\ &= \frac{m_Q^2}{4096\pi^5} \left[\frac{1}{\epsilon} + 10 + \left(64 - \frac{7\pi^2}{4} \right) \epsilon + \mathcal{O}(\epsilon^2) \right], \end{aligned} \quad (\text{A7})$$

$$\begin{aligned} & \mathcal{J}(0, 1, 0, 1, 0, 1, 1, 0, 0) \\ &= \frac{m_Q^4}{8192\pi^5} \left[\frac{1}{\epsilon} + \frac{15}{2} + \left(\frac{145}{4} - \frac{3\pi^2}{4} \right) \epsilon + \mathcal{O}(\epsilon^2) \right], \end{aligned} \quad (\text{A8})$$

$$\begin{aligned} & \mathcal{J}(0, 1, 0, 1, 0, 1, 1, 1, 0) \\ &= \frac{m_Q^2}{8192\pi^5} \left[\frac{1}{\epsilon} + \left(11 - \frac{\pi^2}{3} \right) + \mathcal{O}(\epsilon) \right]. \end{aligned} \quad (\text{A9})$$

APPENDIX B: THE EOM OPERATOR COEFFICIENT

The coefficient \bar{C}_v appears in the matching calculation of the transition operator. The corresponding operator is redundant, and it can be removed by using the EOM.

However, its coefficient is required in the calculation as it shifts the coefficients of higher-order operators. Therefore, presenting its explicit NLO expression might be useful. We split the result as follows:

$$\bar{C}_v = \bar{C}_v^{\text{LO}} + \frac{\alpha_s(\mu)}{\pi} \bar{C}_v^{\text{NLO}}, \quad (\text{B1})$$

with

$$\begin{aligned} \bar{C}_v^{\text{LO}} &= \frac{5}{2} N_c (C_+^2 + C_-^2) + \frac{5}{2} (C_+^2 - C_-^2) \\ &= \frac{15}{2} (C_+^2 + C_-^2) + \frac{5}{2} (C_+^2 - C_-^2), \end{aligned} \quad (\text{B2})$$

$$\begin{aligned} \bar{C}_v^{\text{NLO}} &= -(N_c^2 - 1) \left(\frac{\pi^2}{8} - \frac{65}{96} \right) (C_+^2 + C_-^2) \\ &\quad - \frac{N_c^2 - 1}{2N_c} \left(\frac{15}{2} \ln \left(\frac{\mu^2}{m_Q^2} \right) + \frac{\pi^2}{4} + \frac{1157}{48} \right) (C_+^2 - C_-^2) \\ &= - \left(\pi^2 - \frac{65}{12} \right) (C_+^2 + C_-^2) \\ &\quad - \left(10 \ln \left(\frac{\mu^2}{m_Q^2} \right) + \frac{\pi^2}{3} + \frac{1157}{36} \right) (C_+^2 - C_-^2). \end{aligned} \quad (\text{B3})$$

Note that the color structure is the same that appears in the leading power coefficient. The reason is that one can compute \bar{C}_v by running a small momentum through the diagrams that contribute to C_0 , instead of considering diagrams with one-gluon insertions.

-
- [1] M. A. Shifman and M. B. Voloshin, *Sov. J. Nucl. Phys.* **47**, 511 (1988).
[2] E. Eichten and B. R. Hill, *Phys. Lett. B* **234**, 511 (1990).
[3] N. Isgur and M. B. Wise, *Phys. Lett. B* **232**, 113 (1989).
[4] B. Grinstein, *Nucl. Phys.* **B339**, 253 (1990).
[5] J. Chay, H. Georgi, and B. Grinstein, *Phys. Lett. B* **247**, 399 (1990).
[6] I. I. Y. Bigi, N. G. Uraltsev, and A. I. Vainshtein, *Phys. Lett. B* **293**, 430 (1992); **297**, 477(E) (1992).
[7] B. Blok, L. Koyrakh, M. A. Shifman, and A. I. Vainshtein, *Phys. Rev. D* **49**, 3356 (1994); **50**, 3572(E) (1994).
[8] A. V. Manohar and M. B. Wise, *Phys. Rev. D* **49**, 1310 (1994).
[9] I. I. Y. Bigi, M. A. Shifman, N. G. Uraltsev, and A. I. Vainshtein, *Phys. Rev. Lett.* **71**, 496 (1993).
[10] Y. Amhis *et al.* (HFLAV Collaboration), *Phys. Rev. D* **107**, 052008 (2023).
[11] T. Mannel, D. Moreno, and A. A. Pivovarov, [arXiv:2103.02058](https://arxiv.org/abs/2103.02058).
[12] M. Neubert and C. T. Sachrajda, *Nucl. Phys.* **B483**, 339 (1997).
[13] D. King, A. Lenz, M. L. Piscopo, T. Rauh, A. V. Rusov, and C. Vlahos, *J. High Energy Phys.* **08** (2022) 241.
[14] D. King, A. Lenz, and T. Rauh, *J. High Energy Phys.* **06** (2022) 134.
[15] J. Gratrex, B. Melić, and I. Nišandžić, *J. High Energy Phys.* **07** (2022) 058.
[16] H. Y. Cheng and C. W. Liu, [arXiv:2305.00665](https://arxiv.org/abs/2305.00665).
[17] L. Dulibić, J. Gratrex, B. Melić, and I. Nišandžić, [arXiv:2305.02243](https://arxiv.org/abs/2305.02243).
[18] A. Lenz, *Int. J. Mod. Phys. A* **30**, 1543005 (2015).
[19] H. Y. Cheng, *J. High Energy Phys.* **11** (2018) 014.
[20] A. Lenz, M. L. Piscopo, and A. V. Rusov, *J. High Energy Phys.* **01** (2023) 004.
[21] J. Gratrex, A. Lenz, B. Melić, I. Nišandžić, M. L. Piscopo, and A. V. Rusov, *J. High Energy Phys.* **04** (2023) 034.
[22] M. L. Piscopo, [arXiv:2302.14590](https://arxiv.org/abs/2302.14590).

- [23] M. Fael, K. Schönwald, and M. Steinhauser, *Phys. Rev. D* **104**, 016003 (2021).
- [24] M. Czakon, A. Czarnecki, and M. Dowling, *Phys. Rev. D* **103**, L111301 (2021).
- [25] A. Alberti, P. Gambino, and S. Nandi, *J. High Energy Phys.* **01** (2014) 147.
- [26] T. Mannel, A. A. Pivovarov, and D. Rosenthal, *Phys. Lett. B* **741**, 290 (2015).
- [27] T. Mannel, A. A. Pivovarov, and D. Rosenthal, *Phys. Rev. D* **92**, 054025 (2015).
- [28] A. Lenz and T. Rauh, *Phys. Rev. D* **88**, 034004 (2013).
- [29] T. Mannel and A. A. Pivovarov, *Phys. Rev. D* **100**, 093001 (2019).
- [30] T. Mannel, D. Moreno, and A. A. Pivovarov, *Phys. Rev. D* **105**, 054033 (2022).
- [31] D. Moreno, *Phys. Rev. D* **106**, 114008 (2022).
- [32] B. M. Dassinger, T. Mannel, and S. Turczyk, *J. High Energy Phys.* **03** (2007) 087.
- [33] T. Mannel, S. Turczyk, and N. Uraltsev, *J. High Energy Phys.* **11** (2010) 109.
- [34] G. Altarelli, G. Curci, G. Martinelli, and S. Petrarca, *Nucl. Phys.* **B187**, 461 (1981).
- [35] G. Buchalla, *Nucl. Phys.* **B391**, 501 (1993).
- [36] E. Bagan, P. Ball, V. M. Braun, and P. Gosdzinsky, *Nucl. Phys.* **B432**, 3 (1994).
- [37] F. Krinner, A. Lenz, and T. Rauh, *Nucl. Phys.* **B876**, 31 (2013).
- [38] A. Czarnecki, M. Slusarczyk, and F. V. Tkachov, *Phys. Rev. Lett.* **96**, 171803 (2006).
- [39] B. Blok and M. A. Shifman, *Nucl. Phys.* **B399**, 441 (1993).
- [40] B. Blok and M. A. Shifman, *Nucl. Phys.* **B399**, 459 (1993).
- [41] T. Mannel, D. Moreno, and A. Pivovarov, *J. High Energy Phys.* **08** (2020) 089.
- [42] D. Moreno, *J. High Energy Phys.* **01** (2021) 051.
- [43] A. Lenz, M. L. Piscopo, and A. V. Rusov, *J. High Energy Phys.* **12** (2020) 199.
- [44] M. Beneke, G. Buchalla, C. Greub, A. Lenz, and U. Nierste, *Nucl. Phys.* **B639**, 389 (2002).
- [45] E. Franco, V. Lubicz, F. Mescia, and C. Tarantino, *Nucl. Phys.* **B633**, 212 (2002).
- [46] F. Gabbiani, A. I. Onishchenko, and A. A. Petrov, *Phys. Rev. D* **70**, 094031 (2004).
- [47] A. J. Buras and P. H. Weisz, *Nucl. Phys.* **B333**, 66 (1990).
- [48] M. Jamin and A. Pich, *Nucl. Phys.* **B425**, 15 (1994).
- [49] M. J. Dugan and B. Grinstein, *Phys. Lett. B* **256**, 239 (1991).
- [50] S. Herrlich and U. Nierste, *Nucl. Phys.* **B455**, 39 (1995).
- [51] A. G. Grozin, T. Mannel, and A. A. Pivovarov, *Phys. Rev. D* **98**, 054020 (2018).
- [52] A. G. Grozin, T. Mannel, and A. A. Pivovarov, *Phys. Rev. D* **96**, 074032 (2017).
- [53] A. G. Grozin, R. Klein, T. Mannel, and A. A. Pivovarov, *Phys. Rev. D* **94**, 034024 (2016).
- [54] H. Georgi, *Phys. Lett. B* **240**, 447 (1990).
- [55] T. Mannel, W. Roberts, and Z. Ryzak, *Nucl. Phys.* **B368**, 204 (1992).
- [56] M. Neubert, *Phys. Rep.* **245**, 259 (1994).
- [57] A. V. Manohar, *Phys. Rev. D* **56**, 230 (1997).
- [58] T. Mannel and K. K. Vos, *J. High Energy Phys.* **06** (2018) 115.
- [59] R. N. Lee, arXiv:hep-ph/1212.2685.
- [60] R. N. Lee, *J. Phys. Conf. Ser.* **523**, 012059 (2014).
- [61] M. Jamin and M. E. Lautenbacher, *Comput. Phys. Commun.* **74**, 265 (1993).
- [62] M. Sjö Dahl, *Eur. Phys. J. C* **73**, 2310 (2013).
- [63] T. Huber and D. Maitre, *Comput. Phys. Commun.* **175**, 122 (2006).
- [64] T. Huber and D. Maitre, *Comput. Phys. Commun.* **178**, 755 (2008).
- [65] K. G. Chetyrkin, J. H. Kuhn, and M. Steinhauser, *Comput. Phys. Commun.* **133**, 43 (2000).
- [66] T. Mannel, D. Moreno, and A. A. Pivovarov, *Phys. Rev. D* **104**, 114035 (2021).